**Indonesian Journal of Electronics, Electromedical Engineering, and Medical Informatics** e-ISSN: 2656-8624
Homepage: https://ijeeemi.org/; Vol. 8, No. 1, pp. 56-69, February 2026

RESEARCH PAPER

OPEN ACCES

# MEWT-Enhanced EEGNet for ASD EEG Classification: Performance Evaluation with k-Fold Cross-Validation

**Imam Fathur Rahman[1], Melinda Melinda[1] Yunidar Yunidar[1] , Nurlida Basir[2], and Aufa Rafiki[1]**

[1] Department of Electrical and Computer Engineering, Universitas Syiah Kuala, Banda Aceh, Indonesia
[2] Faculty of Science and Technology, Universiti Sains Islam Malaysia (USIM), Nilai Negeri Sembilan, Malaysia

## Abstract

**Accurate and reliable classification of autism spectrum disorder (ASD) from electroencephalography (EEG) signals remains challenging due to the inherently nonstationary, nonlinear, and multichannel nature of EEG data. These properties complicate the extraction of discriminative features that are both stable and computationally efficient. To address this challenge, this study proposes a compact deep-learning pipeline that integrates the Multivariate Empirical Wavelet Transform (MEWT) with EEGNet for ASD–EEG classification. MEWT decomposes multichannel EEG signals into spectrally aligned subbands while preserving inter-channel relationships. The resulting MEWT-based features are then processed by EEGNet, a lightweight convolutional neural network specifically designed for EEG-based learning tasks. Performance was evaluated using 5-fold cross-validation. The proposed MEWT with the the EEGNet model achieved a mean test accuracy of 98.35%, with consistently high precision (98.23%), recall (98.45%), F1-score (98.34%), and specificity (98.24%) across all folds. Confusion-matrix results indicated very few and well-balanced false positives and false negatives, supporting stable discrimination between ASD and control EEG segments. A one-sample one-tailed t-test against a 50% chance level confirmed that all evaluated metrics were significantly above chance ($p < 0.0001$). When benchmarked against previously reported results on the same dataset, the proposed approach slightly improved upon EMD with EEGNet (97.99%) and clearly outperformed EWT with EEGNet (95.08%), suggesting that MEWT-derived multichannel features are well matched to compact convolutional architectures for ASD–EEG analysis. Despite these strong results, the study is limited by a small, single-site cohort and the use of a single deep-learning model. Future work will focus on standardized retraining across multiple feature families and validation on larger and more diverse populations to further assess robustness and generalizability.**

## Paper History

Received Nov. 18, 2025
Revised Jan. 12, 2026
Accepted Jan. 20, 2026
Published Jan. 27, 2026

## Keywords

Autism spectrum disorder;
Electroencephalography;
Multivariate Empirical Wavelet Transform;
EEGNet;
Cross-validation;
Confusion Matrix

## Author Email

imamfr@mhs.usk.ac.id
melinda@usk.ac.id
yunidar@usk.ac.id
nurlida@usim.edu.my
aufa35@mhs.usk.ac.id

## I. Introduction

Disorders in individuals with ASD are related to changes in the function of the frontal and temporal lobes. In general, increased brain wave activity in the delta to theta frequency band is observed in the frontal area, which is associated with lower cognitive performance [1]. In individuals with ASD, alpha wave activity, commonly associated with relaxation, tends to be lower, while beta wave activity, associated with focus and attention, tends to be higher. This oscillation pattern suggests that brain wave dynamics may play a role in the developmental mechanisms of ASD [2]. Recent reviews and meta-analyses suggest that ASD-related EEG findings are heterogeneous, encompassing band-specific power alterations in delta, theta, alpha, and beta ranges, atypical functional connectivity patterns, and changes in signal complexity. Reported effects also appear to be moderated by factors such as age, behavioral state during recording, and acquisition protocols. Collectively, these observations motivate feature representations that are physiologically interpretable in the spectral domain while remaining robust to cross-channel variability and protocol-related differences [3],[4].

Brain activity can be studied through functional imaging, which measures brain signals using EEG (Electroencephalography)[5]. EEG is a method for recording the brain's spontaneous electrical activity, arising from the transmission of signals between neurons. Recording is generally performed for short durations, around 20-40 minutes, by placing electrodes at several points on the scalp [6]. EEG signals require feature extraction to convert raw signals into meaningful indicators of information. These features enable analysis and classification in various applications, such as emotion recognition, BCI, seizure detection, and ASD identification [7]. The feature extraction process generally includes preprocessing, decomposition, and then the extraction of relevant features from the processed signal. Various

**Corresponding author:** Melinda, melinda@usk.ac.id, Department of Electrical and Computer Engineering, Universitas Syiah Kuala, Banda Aceh, Indonesia.
**Digital Object Identifier (DOI):** https://doi.org/10.35882/ijeeemi.v8i1.313

approaches can be used, such as statistical measures, time–frequency analysis, and advanced decomposition techniques such as Multivariate Empirical Wavelet Transform (MEWT) [8].

On the same dataset, a prior study used the Empirical Wavelet Transform (EWT) with EEGNet to classify ASD vs. non-ASD subjects, achieving an average test accuracy of 95.08% [9]. Nevertheless, EWT was applied univariately (per channel), meaning that frequency-band boundaries could differ across channels; consequently, cross-channel consistency and synchronization information may not be optimally preserved. Motivated by this limitation, this work replaces EWT with MEWT while retaining EEGNet as the classifier, aiming to produce time–frequency representations that are more consistent across channels for ASD detection [9]. MEWT decomposes multichannel signals into a set of multivariate wavelet coefficients that capture time and frequency information simultaneously across all channels [10]. Unlike univariate decompositions, MEWT jointly determines band boundaries across channels, so that each channel is analyzed under an identical frequency partition. This property is particularly relevant for EEG, where synchronous patterns across channels may carry discriminative information; therefore, MEWT is expected to improve the stability and reliability of extracted time-frequency features in multichannel ASD EEG analysis [11]. MEWT extends univariate EWT by deriving a single, data-driven empirical wavelet filter bank from a representative multichannel spectrum and applying it uniformly across channels, thereby promoting multichannel-consistent, spectrally aligned sub-bands. EEGNet complements this representation through temporal convolutions that learn local time patterns and depthwise spatial convolutions that model inter-channel coordination with very few trainable parameters, making it suitable for compact, screening-oriented EEG pipelines [12], [13]

The next step is classification modeling to map MEWT vectors to ASD and normal labels. This study selected one deep learning model paradigm, namely, EEGNet [14]. EEGNet is selected for three main reasons: (i) it is effective for modeling nonlinear and noisy EEG characteristics, (ii) it is computationally efficient for controlled training and validation, and (iii) it has demonstrated strong performance across diverse EEG tasks when evaluated under proper validation protocols [12]. Architecturally, EEGNet captures temporal patterns via temporal convolutions, models inter-channel coordination through depthwise spatial convolutions, and reduces parameter complexity using separable convolutions without substantially sacrificing representational capacity[13]. Accordingly, this work evaluates performance using Accuracy, Precision, Recall, F1-score, and Specificity, complemented by inferential assessment. Based on this background, the objectives of this study are to: (i) evaluate the ability of MEWT to generate stable and consistent time–frequency features across channels in a multichannel ASD EEG dataset, and (ii) assess the performance of the MEWT–EEGNet combination in distinguishing ASD and non-ASD subjects at the subject level using rigorous subject-wise validation.

The contributions of this study are as follows: 1) We propose an ASD EEG classification pipeline that replaces univariate EWT with multichannel-consistent MEWT to improve cross-channel alignment of time–frequency representations, 2) We integrate MEWT features with EEGNet to simultaneously model temporal and spatial EEG patterns using a compact and computationally efficient CNN architecture, 3) We provide a subject-wise K-fold evaluation protocol to prevent intra-subject leakage and report comprehensive metrics (Accuracy, Precision, Recall, F1-score, and Specificity) to characterize performance robustness across individuals.

This paper is organized as follows: This paper is organized as follows: Section I introduces the research background, problem formulation, and main contributions of this study. Section II reviews the materials and methodological background, including EEG preprocessing, MEWT, and EEGNet. Section III describes the results. Section IV presents the experimental results and discusses the comparative findings. Finally, Section V concludes the paper and outlines future work.

## II. Materials and Method

Fig. 1 summarizes the workflow of this study. The data come from the Primer EEG dataset, consisting of 10 subjects (5 with ASD, 5 controls) recorded with 16 channels at a sampling frequency of 250 Hz. Raw EEG signals were visually checked, then preprocessed using a zero-phase 0.5–40 Hz Butterworth band-pass filter, and segmented into fixed-length epochs that served as individual samples. For feature extraction, the preprocessed multichannel EEG was decomposed using Multivariate Empirical Wavelet Transform (MEWT). A representative multichannel spectrum was used to design a common empirical wavelet filter bank, ensuring consistent frequency bands for all channels. The resulting MEWT filter bank was applied uniformly to each channel to obtain spectrally aligned sub-bands; these sub-bands were then summed to reconstruct a denoised multichannel signal per subject. The denoised EEG was segmented into fixed-length epochs and used as input to EEGNet for end-to-end classification. Performance was reported with subject-wise 5-fold cross-validation and fold-level metrics (Accuracy, Precision, Recall, F1-score, and Specificity).

All data were split into 80% training and 20% test data under a subject-wise 5-fold cross-validation scheme, so that epochs from the same subject did not appear in both training and test sets within a fold. The classification stage used EEGNet with the Adamax optimizer, a learning rate of 0.001, a batch size of 64, 50 training epochs, and binary cross-entropy loss. For each fold, the model was trained on the training set and evaluated on the test set. Performance was assessed using learning curves (training/validation accuracy and loss), the confusion matrix (TP, FP, FN, TN), and the metrics Accuracy, Precision, Recall, F1-score, and Specificity across folds.

**Corresponding author:** Melinda, melinda@usk.ac.id, Department of Electrical and Computer Engineering, Universitas Syiah Kuala, Banda Aceh, Indonesia.
**Digital Object Identifier (DOI):** https://doi.org/10.35882/ijeeemi.v8i1.313

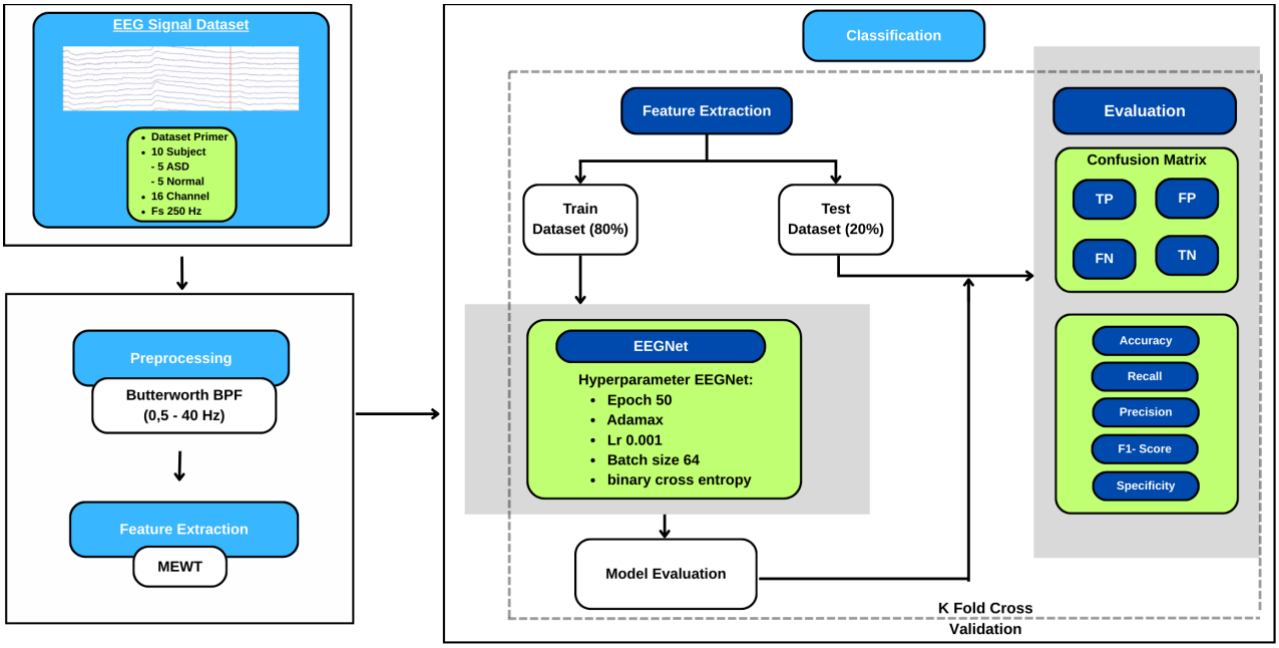


**Fig. 1. Block diagram of preprocessing, MEWT feature extraction, and EEGNet classification**

### A. Dataset

The materials required for this study were EEG signal datasets, consisting of raw EEG data from individuals with ASD and from normal individuals, acquired directly from subjects using the Open BCI Cyton Board. EEG data were collected from ten participants in Banda Aceh, Indonesia, who were divided into two groups. The first group consisted of five adolescents and young adults aged 15 to 25 years with Autism Spectrum Disorder (ASD) recruited from local special schools, while the second group consisted of five neurotypical individuals aged 17 to 25 years living around Syiah Kuala University. Data collection was conducted in a quiet and controlled room between 9:00 a.m. and 12:00 p.m. to keep participants calm and cooperative. Each session lasted approximately 40 minutes, including 10 minutes for preparation and electrode placement, and two 15-minute recording sessions [15]. All research procedures have been approved by the Ethics Committee with reference number 117/EA/FK/2024 and are declared to be in accordance with the WHO 2011 standards. The dataset used in this study involves 16 channels, which represent the location of electrode placement on the scalp during the EEG signal acquisition process. The electrode placement consisted of the Frontal (front of the brain) section, which included channels Fp1, Fp2, F7, F3, Fz, F4, and F8. The Temporal (middle side) section included channels T3 and T5. The Central (top center) section included channels C3, C4, and Cz. Finally, the Parietal (upper back) and Occipital (lower back) sections include channels Pz, O1, and Oz [16].

### B. Butterworth Band Pass Filter

A Butterworth band-pass filter is a filter with a flat maximum magnitude response in the passband, so that the signal amplitude within a certain frequency range remains flat [17]. This filter is formed from a combination of high-pass and low-pass filters, so that only frequencies between the two cut-off frequencies are passed, while frequencies outside that range are attenuated [18]. Its characteristics are that the amplitude is very flat in the band-pass, but the phase response is not linear, so the phase change depends on the signal frequency [17]. In this study, EEG recordings were acquired at a sampling rate of 250 Hz, and all 16 available channels were included in the analysis. During preprocessing, each channel was passed through a 4th-order Butterworth band-pass filter with cut-off frequencies of 0.5 and 40 Hz. This type of filter was chosen because its maximally flat passband magnitude helps maintain the original waveform with minimal distortion [19]. The 0.5–40 Hz range spans the principal EEG rhythms delta, theta, alpha, beta, and part of the low-gamma band while simultaneously suppressing very slow components caused by drift and body movements, as well as higher-frequency disturbances from muscle activity and environmental noise. These settings were tailored to the spectral characteristics of EEG signals, ensuring that subsequent feature extraction and classification stageoperate on clean, informative signals. Similar pass-band choices (0.5–40 Hz) are widely used to mitigate drift and EMG contamination and to stabilize downstream decoding performance across preprocessing settings. [20], [21].

After preprocessing, each subject's continuous EEG was segmented into fixed-length epochs of 2 s (500 samples at 250 Hz) with 50% overlap. A 2-s epoch is a practical trade-off: it is short enough to approximate local stationarity and increase the number of training samples, yet long enough to preserve the oscillatory dynamics commonly reported in ASD EEG studies. A 50% overlap

**Corresponding author:** Melinda, melinda@usk.ac.id, Department of Electrical and Computer Engineering, Universitas Syiah Kuala, Banda Aceh, Indonesia.
**Digital Object Identifier (DOI):** https://doi.org/10.35882/ijeeemi.v8i1.313

improves temporal coverage while limiting redundancy relative to higher-overlap settings [22], [23]. Because overlapping epochs from the same subject are highly correlated, we used subject-wise cross-validation to prevent identity confounding and data leakage when forming train and test splits [24], [25].

### C. Multivariate Empirical Wavelet Transform

The Multivariate Empirical Wavelet Transform (MEWT) is a multichannel generalization of the Empirical Wavelet Transform (EWT) that decomposes multivariate signals using a single, data-driven set of frequency boundaries shared across channels. Unlike univariate EWT, which estimates spectral boundaries independently for each channel, MEWT first analyzes the joint multichannel Fourier spectrum of an EEG trial to identify salient spectral transitions and define a common partition of the frequency axis [26], [11]. These empirically determined band limits are computed once per trial (or per dataset, depending on the implementation) and then used to construct an adaptive wavelet filter bank, which is applied identically to every channel. As a result, the extracted sub-bands are spectrally co-registered across electrodes, facilitating direct cross-channel comparison and stabilizing multichannel learning, while preserving the smooth, tight-frame reconstruction properties and adaptivity that characterize EWT [27],[28],[29].

1. Fourier Transform & Multichannel Spectral Aggregation

The first step is to transform the EEG signal into the frequency domain. For each EEG channel $x_c(t)$, with $c = 1, \dots, C,$) the Fast Fourier Transform (FFT) is calculated in Eq. (1) [30]:

$$\widehat{X_c}(\omega) = \mathcal{F} x_c(t) \tag{1}$$

The spectrum $\hat{X}_c(\omega)$ describes how the energy of the channel $c$ is distributed at a frequency $\omega$. o obtain a combined spectral representation of all channels, a composite spectrum $S(\omega)$ is formed using two commonly used forms, Eq. (2) [29] and Eq. (3) [29]:

(i) Average spectral magnitude

$$\bar{S}(\omega) = \frac{1}{C}\sum_{c=1}^{C}\left|\widehat{X_c}(\omega)\right| \tag{2}$$

(ii) Spectral root-sum-of-squares (energy)

$$\bar{S}(\omega) = \left(\sum_{c=1}^{C}\left|\widehat{X_c}(\omega)\right|^2\right)^{1/2} \tag{3}$$

The combined spectrum $\bar{S}(\omega)$ is then smoothed to stabilize peak and valley detection. The frequency domain $[0, \omega_{\mathrm{Nyq}}]$ is then segmented into $K$ bands with boundaries $\Omega = \{\omega_1, \dots, \omega_K\}$ obtained through local peak searches on $\bar{S}(\omega)$ nd boundary placement at the midpoint between peaks. This mechanism underlies the adaptive nature of MEWT compared to non-adaptive wavelet systems [28],[29]. In this study, we constructed the representative multichannel spectrum using the spectral root-sum-of-squares formulation (Eq. (3)) [29], which emphasizes shared spectral peaks across channels and has been adopted in multidimensional empirical wavelet transform implementations for multichannel EEG.

2. Meyer-like Window Construction (Scaling & Wavelet)

After the band limits are determined, a scaling function and wavelet function (Meyer-like windows) are constructed in the frequency domain (Eq. (4)) [29]. The scaling $\widehat{\varphi_0}(\omega)$ covers low frequencies, while the wavelet $\widehat{\psi_k}(\omega)$ is active in the range $[\omega_k, \omega_{k+1}]$ with smooth edges (roll-off).

$$\{\widehat{\varphi_0}(\omega), \widehat{\psi_k}(\omega)\}_{k=1}^{K} \tag{4}$$

Smooth transitions between bands ensure that the filter bank does not abruptly cut off the spectrum, but ratherinstead forms a stable, redundant empirical wavelet frame. Because the shapes of $\hat{\varphi}_0(\omega)$ and $\hat{\psi}_k(\omega)$ follow the spectrum structure $S(\omega)$ obtained from the data, this filter bank is empirical and adaptive, unlike conventional wavelets that depend on predefined scale and translation parameters [29],[31].

3. Cross-Channel Uniform Subband Projection

The bank filter formed is then applied uniformly to each EEG channel, so that each channel has a subband with identical frequency limits. The projection for channel -$c$ is given by Eq. (5) [32]:

$$\begin{aligned} x_{c,0}(t) &= \mathcal{F}^{-1}\widehat{\varphi_0}(\omega)\,\widehat{X_c}(\omega) \\ x_{c,k}(t) &= \mathcal{F}^{-1}\widehat{\psi_k}(\omega)\,\widehat{X_c}(\omega), k = 1, \dots, K \end{aligned} \tag{5}$$

This decomposition produces a set of subband signals for each channel with a consistent band structure across channels. This configuration allows features such as energy, spectral entropy, and center frequency (centroid) to be calculated for each subband and directly compared across channels and subjects in the same frequency domain [29], [32].

### D. EEGNet

EEGNet is a compact CNN designed for EEG classification that organizes feature learning into three core stages Fig. 2: temporal filtering, spatial filtering per temporal feature (capturing inter-channel relationships), and efficient feature fusion via separable convolution [9], [12], [14], [33]. Mathematically, the first stage applies a time-domain convolution to each channel to produce temporal feature maps (Eq. (6)) [12]:

$$Z_f(c,t) = \sum_{\tau=1}^{L} W_{f,\tau}^{(1)}\; X(c, t+\tau-1) + b_f \tag{6}$$

In Eq. (6) [12], where $X(c,t)$denotes the EEG sample from channel $c$at time $t$, $L$is the temporal kernel length, $W^{(1)}$are the kernel weights, and $b_f$is the bias term [34]. Next, DepthwiseConv2D acts as a spatial filter that aggregates information across channels for each temporal feature map separately:

$$Y_f(t) = \sum_{c=1}^{C} W_{f,c}^{(2)}\; Z_f(c,t) \tag{7}$$

**Corresponding author:** Melinda, melinda@usk.ac.id, Department of Electrical and Computer Engineering, Universitas Syiah Kuala, Banda Aceh, Indonesia.
**Digital Object Identifier (DOI):** https://doi.org/10.35882/ijeeemi.v8i1.313

In Eq. (7) [12], where $C$is the number of channels and $W^{(2)}$are the spatial-filter weights [12]. Finally, SeparableConv2D compresses and combines the resulting feature maps into a more compact representation by merging information across features (Eq. (8)) [12]:

$$U_k(t) = \sum_{f=1}^{F} W_{k,f}^{(3)}\ Y_f(t) + b_k \qquad (8)$$

In Eq. (8) [12], where $W^{(3)}$are the fusion weights, $b_k$is the bias, and $k$ indexes the final filters. The resulting features are then passed to a pooling and a classification layer to produce the final decision [9]. EEGNet configuration used in this study follows a compact EEGNet-style design. We employed three successive convolutional stages with 8, 4, and 2 filters and kernel sizes of 1 × 32, 2 × 16, and 8 × 4, respectively. Each stage was followed by ELU activation and batch normalization. Temporal downsampling was performed using max-pooling with a pool size of 1 × 4 after the second and third stages, while zero-padding along the time dimension was applied to maintain adequate temporal coverage.

The resulting feature maps were flattened and passed to a single fully connected neuron with a sigmoid activation to produce a binary output. Training in each fold was conducted for up to 50 epochs using the Adamax optimizer and binary cross-entropy loss. The compactness of EEGNet (0,001 trainable parameters in common configurations) has been widely reported, supporting its suitability for resource-constrained deployment [12]

### E. K-Fold Cross Validation

K-Fold cross-validation is one of the most commonly used cross-validation techniques in machine learning to measure overall model performance. This method works by dividing the dataset into k subsets or folds of similar size; then the model is trained on $k$ -1 folds and tested on the remaining fold. This process is repeated k times, so that all data is used in turn for training and testing. The average value of all test results is then used as an indicator of the overall performance of the model [35], [36]. Mathematically, if $D = \{(x_i, y_i)\}_{i=1}^{n}$ is a dataset with n samples, and $D_j$ s the jth subset of $k$ -fold, then the average accuracy can be expressed as Eq. (9) [35]:

$$\text{Accuracy}_{\text{avg}} = \frac{1}{k}\sum_{j=1}^{k} \text{Accuracy}\,(M^{-j}, D_j), \qquad (9)$$

In Eq. (9) [35], where $M^{-j}$ is the model trained on all data except fold -$j$, and $D_j$ is the validation data. Recent studies show that the use of K-Fold Cross-Validation can reduce the risk of overfitting and improve the stability of generalization for EEG signal classification models [35], [36], [37]. In this work, we implemented a subject-wise 5-fold cross-validation scheme: the 10 subjects (5 ASD, 5 control) were partitioned into five folds, with each fold holding out 2 subjects (1 ASD and 1 control), corresponding to approximately 20% of the subjects for testing, while the remaining 8 subjects (80%) were used for training. All epochs generated from a held-out subject were kept exclusively in the test set for that fold. This design is recommended for EEG deep learning studies because random segment-level splits can substantially

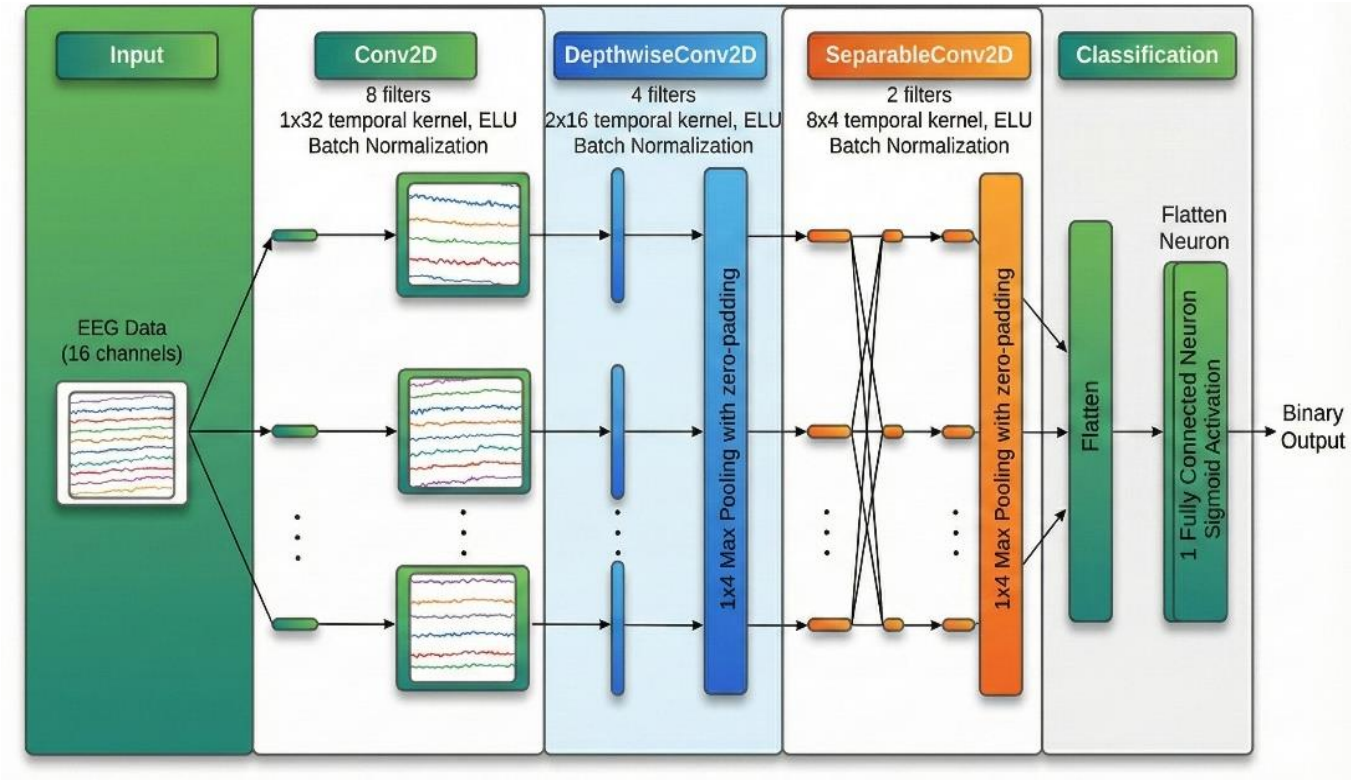


**Fig. 2. Schematic diagram of the EEGNet model for EEG signal classification**

**Corresponding author:** Melinda, melinda@usk.ac.id, Department of Electrical and Computer Engineering, Universitas Syiah Kuala, Banda Aceh, Indonesia.
**Digital Object Identifier (DOI):** https://doi.org/10.35882/ijeeemi.v8i1.313

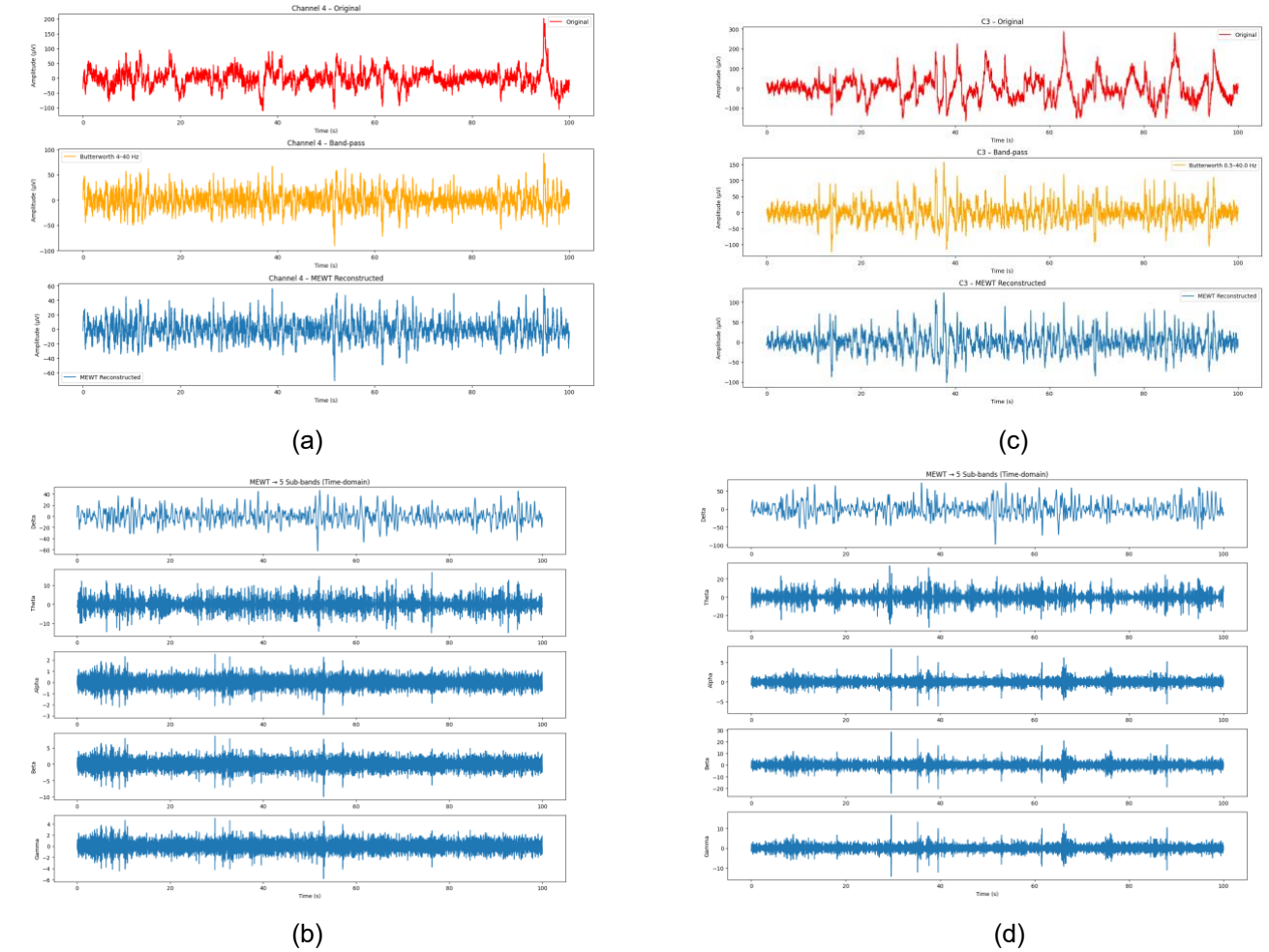


**Fig. 3. Time domain MEWT visualization: (a) raw EEG signal, band-pass filtered signal ASD, and MEWT-reconstructed signal, (b) five ASD MEWT sub-band, (c) raw EEG signal, band-pass filtered signal NORMAL, and MEWT-reconstructed signal, (d) five NORMAL MEWT sub-band**

overestimate performance when subject identity leaks across folds. [24], [25]. A confusion matrix is used to evaluate the performance of machine learning and deep learning models by displaying a summary of prediction results in matrix form, enabling evaluation metrics such as accuracy, precision, recall, and specificity to be calculated systematically [38],[39]. A confusion matrix generally consists of four components, namely TP (true positive), FP (false positive), TN (true negative), and FN (false negative) [40].

## III. Results

### A. Butterworth Band Pass

In the first preprocessing step, the EEG is restricted to the conventional analysis band using a Butterworth band-pass filter with cut-off frequencies of 0,5–40 Hz (middle panel, orange trace). The upper panel of Fig.3 displays the raw Channel-4 (C3) recording (red), which still contains large, slow drifts and sporadic high-amplitude spikes, with values ranging roughly from −100 to 200 µV. These fluctuations reflect a mixture of ocular, movement, and environmental artifacts that mask the underlying cortical rhythms and yield a highly unstable baseline. After applying the 4–40 Hz Butterworth filter, the waveform in the middle panel becomes more compact and regular, with amplitudes confined to about −80 to 80 µV. Low-frequency baseline wander and very high-frequency noise are strongly attenuated, while oscillatory activity in the classical EEG bands is preserved. Because the Butterworth filter has a maximally flat magnitude response in the passband, it suppresses out-of-band components without introducing ripples, thereby maintaining the essential temporal structure required for subsequent multichannel processing

### B. MEWT

The bottom panel of Fig. 3 (a) shows the same channel after Multivariate Empirical Wavelet Transform (MEWT) decomposition and reconstruction (blue trace). Following the decomposition stage, the five resulting components are recombined by time-domain aggregation to form a reconstructed signal for each channel. When minor length mismatches arise from padding operations or rounding in index computations, a one-dimensional linear interpolation step is used to resample the reconstruction to match the original signal duration. This reconstruction procedure further suppresses remaining ocular and EMG-

**Corresponding author:** Melinda, melinda@usk.ac.id, Department of Electrical and Computer Engineering, Universitas Syiah Kuala, Banda Aceh, Indonesia.
**Digital Object Identifier (DOI):** https://doi.org/10.35882/ijeeemi.v8i1.313

related artifacts beyond what band-pass filtering alone can remove, while maintaining the essential waveform structure prior to classification.

MEWT is applied jointly to all EEG channels. The combined multichannel spectrum of each trial is used to derive adaptive frequency boundaries that define five non-overlapping sub-bands associated with delta, theta, alpha, beta, and gamma activity. The same empirically derived wavelet filter bank is then applied to every channel, ensuring that sub-band contents are aligned across the 16 electrodes. For the ASD example in Channel 4 shown in Fig. 3(a), the raw EEG is plotted over approximately −200 to 200 μV, the Butterworth band-pass-filtered signal is shown over approximately −100 to 100 μV, and the MEWT-reconstructed signal is further compressed to approximately −80 to 60 μV. The reconstructed waveform becomes more regular and clearly oscillatory than the band-pass-only output, indicating an improved signal-to-noise ratio. Slow drifts and sharp muscle-related transients that survive conventional band-pass filtering are largely reduced, while the morphology of the underlying cortical rhythms is preserved. The MEWT-reconstructed signals, therefore, provide cleaner, more consistent input for downstream feature extraction and ASD classification.

The corresponding MEWT sub-bands for Channel 4 are displayed in Fig. 3 (b). From top to bottom, the panels show the delta, theta, alpha, beta, and gamma components in the time domain. The delta component spans approximately −40 to 40 μV, theta spans approximately −20 to 20 μV, alpha spans approximately −8 to 8 μV, beta spans approximately −8 to 8 μV, and gamma spans approximately −3 to 3 μV. These differences in vertical scale highlight the natural attenuation of signal energy with increasing frequency and confirm that MEWT distributes EEG power into physiologically meaningful delta–gamma components that sum to the reconstructed waveform in Fig. 3 (a). For Channel C3 in the normal example shown in Fig. 3 (c), the same procedure produces five sub-band signals whose sum yields a near-perfect reconstruction of the Butterworth-filtered EEG, with substantially reduced residual artifacts. The raw EEG is plotted over approximately −200 to 200 μV, the band-pass filtered signal is shown over approximately −150 to 150 μV, and the MEWT-reconstructed signal is further compressed to approximately −60 to 60 μV. The reconstructed waveform appears more regular and clearly oscillatory, indicating improved signal-to-noise ratio compared with the band-pass-only output. The corresponding MEWT sub-bands for Channel C3 are displayed in Fig. 3 (d), where the first component spans approximately −100 to 50 μV, the second spans approximately −20 to 20 μV, and the remaining components are plotted over approximately −10 to 10 μV, confirming that MEWT separates the signal into aligned sub-band contributions that sum back to the reconstructed waveform in Fig. 3 (c).

### C. EEGNet Result with MEWT

In this study, EEG classification is performed using a compact convolutional neural network inspired by EEGNet, applied to preprocessed and segmented EEG signals. After band-pass filtering and applying the MEWT method, each recording is cut into 2-s windows with 50% overlap, and every 16-channel window (16 × 500) is linearly resampled along the temporal axis to obtain a uniform input size of 16 × 1000 samples, resulting in a total of 8940 overlapping EEG snapshots used to train and evaluate the model. The resulting segments are evaluated using a 5-fold cross-validation scheme implemented with shuffled splits. For each split, approximately 80% of the segments are used for training, and the remaining 20% for testing. A new network is initialized and trained from scratch so that no parameters are shared across folds. The test accuracy across each fold is then averaged to summarize the model's generalization performance.

**Table 1. The EEGNet Train Test Accuracy Using Five-Fold Cross-Validation**

| Fold | Train Acc (%) | Test Acc (%) |
|---|---|---|
| Fold 1 | 98.90 | 98.72 |
| Fold 2 | 98.83 | 98.94 |
| Fold 3 | 99.04 | 98.16 |
| Fold 4 | 97.69 | 97.77 |
| Fold 5 | 98.48 | 98.16 |

The EEGNet implementation adopted here consists of three successive convolutional stages with 8, 4, and 2 filters and temporal kernel sizes of 1 × 32, 2 × 16, and 8 × 4, respectively. Each stage is followed by ELU activation and batch normalization, while 1 × 4 max-pooling is applied after the second and third stages with zero-padding along the time dimension to preserve sufficient temporal coverage. The final feature maps are flattened and connected to a single fully connected neuron with sigmoid activation to produce a binary output. Training in each fold is performed for up to 50 epochs using the Adamax optimizer and binary cross-entropy loss, with classification accuracy on the held-out fold serving as the primary evaluation metric. The performance of EEGNet when trained on MEWT-based features is summarized in Table 1. The training accuracies for the five folds are 98.90%, 98.83%, 99.04%, 97.96%, and 98.48%, respectively, while the corresponding testing accuracies are 98.72%, 98.94%, 98.16%, 97.77%, and 98.16%.

The mean training and testing accuracies reach 98.64% and 98.35%, respectively, indicating that the network consistently learns the MEWT feature representation without severe overfitting and maintains very high generalization performance across different partitions of the data. In addition to accuracy, the detailed per-fold metrics for EEGNet with MEWT are reported in Table 2. Across the five folds, accuracy ranges from

**Corresponding author:** Melinda, melinda@usk.ac.id, Department of Electrical and Computer Engineering, Universitas Syiah Kuala, Banda Aceh, Indonesia.
**Digital Object Identifier (DOI):** https://doi.org/10.35882/ijeeemi.v8i1.313

97.77% to 98.94%, with Precision ranging from 97.70% to 98.77% and Recall ranging from 97.32% to 99.68%. The F1-Score remains high and stable (97.76%–98.98%), while Specificity lies between 97.84% and 98.22%. The mean values over all folds reach 98.35% for Accuracy, 98.24% for Precision, 98.45% for Recall, 98.34% for F1-Score, and 98.24% for Specificity, with an average AUC of 99.86%. These results show that the model not only achieves excellent overall accuracy but also balanced performance in correctly identifying both normal and ASD classes. To further characterize the classification behavior of the model, the confusion matrices for all five folds are presented in Fig. 4. In every fold, the diagonal entries (true normal and true ASD) clearly dominate the off-diagonal ones, indicating that the EEGNet with MEWT model correctly classifies the vast majority of EEG segments for both classes. Among these, Fold 2 exhibits the most favorable pattern, with only 19 misclassified samples out of 1,791 test instances, which corresponds to an error rate of approximately 1.1%. In this fold, 846 normal samples are correctly predicted as normal, and only 16 are erroneously labeled as ASD, while 926 ASD samples are correctly identified, and only 3 are predicted as normal. Thus, false positives and false negatives are both very rare and remain well balanced.

**Table 2. EEGNet MEWT Fold-Level EEG Classification Performance Using Five-Fold Cross-Validation Metric**

| Fold | Acc (%) | Prec (%) | Rec (%) | F1 (%) | Spec (%) |
|---|---|---|---|---|---|
| Fold 1 | 98.72 | 98.77 | 98.66 | 98.72 | 98.77 |
| Fold 2 | 98.94 | 98.30 | 99.68 | 98.98 | 98.14 |
| Fold 3 | 98.16 | 97.70 | 98.50 | 98.10 | 97.84 |
| Fold 4 | 97.77 | 98.20 | 97.32 | 97.76 | 98.21 |
| Fold 5 | 98.16 | 98.20 | 98.09 | 98.15 | 98.22 |

This balanced error distribution is important in the medical context (Table 2) because it shows that the model does not strongly favor one class over the other; it is able to maintain high sensitivity to ASD cases (low miss rate) without sacrificing specificity for normal subjects (low false-alarm rate). Similar patterns, with slightly higher but still small numbers of misclassifications, are observed in the other folds, reinforcing the conclusion that the EEGNet–MEWT model is stable across different test subsets. Overall, the confusion-matrix analysis confirms that the proposed model is not only accurate in aggregate metrics, but also reliable and well-calibrated in distinguishing normal and ASD EEG segments, making it suitable as a supportive tool for clinical decision-making in ASD detection

### D. Statistical Test (One-Sample t-Test)

As shown in Table 3, all performance metrics lie in a very high range and are consistent across folds. The mean accuracy across folds reaches 98.35 ± 0.47%, with precision of 98.23 ± 0.38%, recall of 98.45 ± 0.86%, F1-score of 98.34 ± 0.50%, and specificity of 98.24 ± 0.34%. Standard deviations below 1% across all metrics indicate that the variation in performance due to data partitioning within each fold is relatively small, suggesting that the model is stable with respect to changes in the training and test subsets. Inferentially, a one-sample t-test (Table 3) was conducted to examine whether the mean classification performance was significantly above the 50% chance level (balanced two-class problem). For accuracy, the test yielded $t(4) = 228.74$, $p < 0.0001$ (one-tailed), confirming that the mean accuracy of 98.35% is well beyond random performance. Similar results were obtained for the other metrics: precision ($t(4) = 283.45$, $p < 0.0001$), recall ($t(4) = 125.81$, $p < 0.0001$), F1-score ($t(4) = 217.93$, $p < 0.0001$), and specificity ($t(4) = 320.82$, $p < 0.0001$). Thus, all performance metrics exhibit highly significant differences relative to chance. Taken together, these findings indicate that the combination of MEWT as a feature extraction method and EEGNet as the classifier can discriminate between ASD and normal subjects with very high.

**Table 3. Fold Averaged Metrics of EEGNet with MEWT (5-Fold CV) and One-Sample t-Test.**

| Metric | Mean ± SD (%) | t (4) | p (one-tailed vs 50%) |
|---|---|---|---|
| Accuracy | 98.35 ± 0.47 | 228.74 | < 0.0001 |
| Precision | 98.23 ± 0.38 | 283.45 | < 0.0001 |
| Recall | 98.45 ± 0.86 | 125.81 | < 0.0001 |
| F1-score | 98.34 ± 0.50 | 217.93 | < 0.0001 |
| Specificity | 98.24 ± 0.34 | 320.82 | < 0.0001 |

**Table 4. EEGNet Benchmark Performance Comparison Across Multiple Evaluation Scenarios**

| Method | Mean Test Accuracy (%) |
|---|---|
| EWT with EEGNet [9] | 95.08 |
| EMD with EEGNet [9] | 97.99 |
| MEWT with EEGNet (proposed Method) | 98.35 |

## IV. Discussion

In this study, we focused on evaluating a new MEWT with an EEGNet pipeline for ASD–EEG classification. The proposed model, trained on 16-channel EEG segments (2-s windows, 50% overlap, 16 × 1000 input), achieved a mean test accuracy of 98.35%, with high and stable precision, recall, F1-score, specificity, and AUC across the five folds. The confusion matrices show that the MEWT-based model produces very few, well-balanced false positives and false negatives, indicating reliable separation between ASD and normal segments. To verify

**Corresponding author:** Melinda, melinda@usk.ac.id, Department of Electrical and Computer Engineering, Universitas Syiah Kuala, Banda Aceh, Indonesia.
**Digital Object Identifier (DOI):** https://doi.org/10.35882/ijeeemi.v8i1.313

that this performance is genuinely above chance, a one-

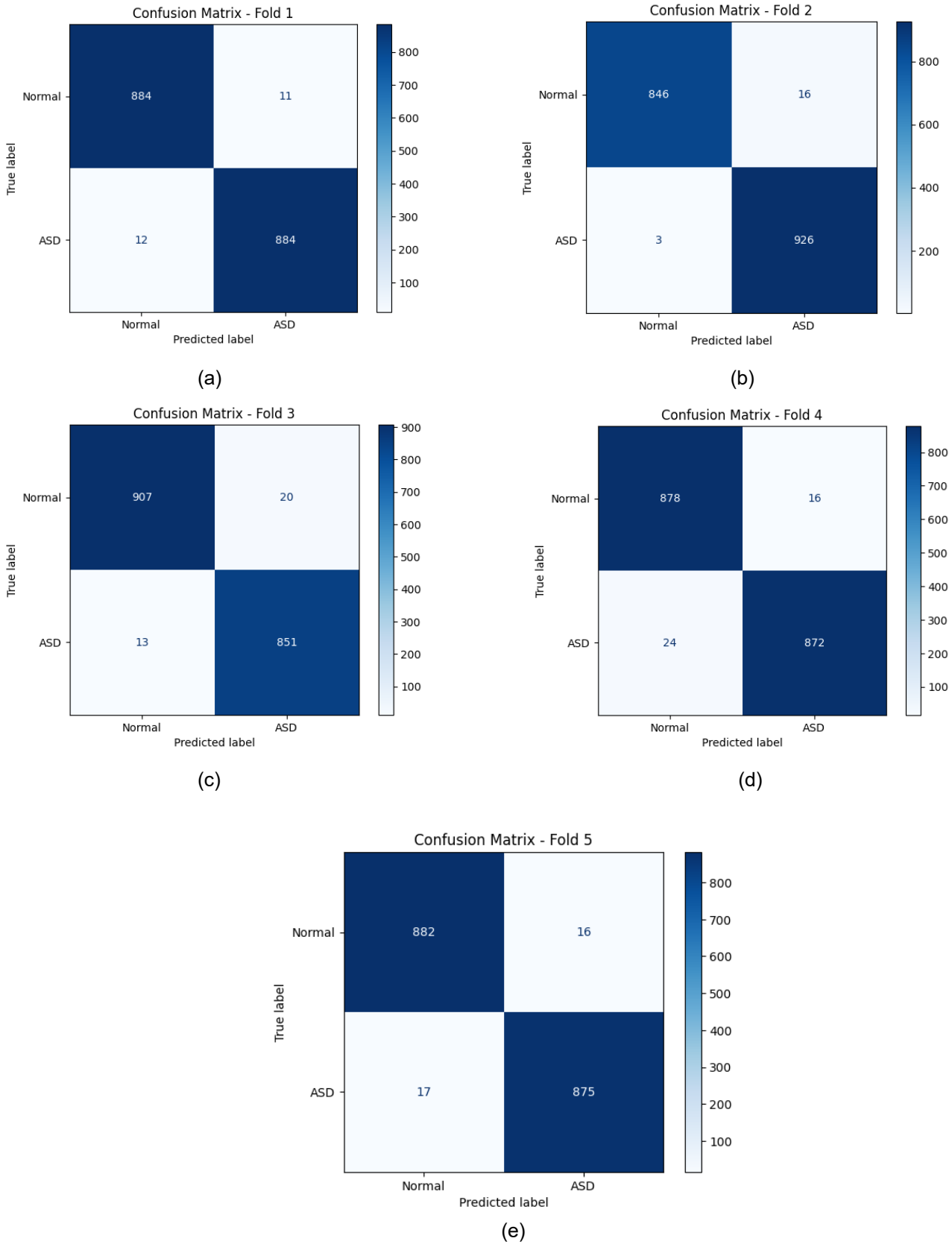


**Fig. 4. Confusion matrices for each fold in 5-fold cross-validation: (a) Fold 1, (b) Fold 2, (c) Fold 3, (d) Fold 4, (e) Fold 5**

**Corresponding author:** Melinda, melinda@usk.ac.id, Department of Electrical and Computer Engineering, Universitas Syiah Kuala, Banda Aceh, Indonesia.
**Digital Object Identifier (DOI):** https://doi.org/10.35882/ijeeemi.v8i1.313

sample t-test against the 50% chance level (balanced two-class setting) was conducted on the five folds. For accuracy, the test yielded $t(4) = 228.74$with $p < 0.0001$(one-tailed), confirming that the mean accuracy of 98.35% is far beyond random performance. Similar results were obtained for precision $(t(4) = 283.45, p < 0.0001)$, recall $(t(4) = 125.81, p < 0.0001)$, F1-score $(t(4) = 217.93, p < 0.0001)$, and specificity $(t(4) = 320.82, p < 0.0001)$, showing that all metrics are significantly higher than the chance baseline

For context, the proposed MEWT with the EEGNet method is benchmarked against the previous study [9]. on the same ASD EEG dataset, which employed EWT and EMD-based features with EEGNet under a subject-wise 5-fold cross-validation scheme. The earlier work reported mean test accuracies of 95.08% for EWT with EEGNet and 97.99% for EMD with EEGNet [9]. As summarized in Table 4, the proposed MEWT with the EEGNet pipeline improves the EWT-based baseline by 3.27 percentage points (95.08% → 98.35%) and slightly outperforms the EMD-based baseline by 0.36 percentage points (97.99% → 98.35%). These gains suggest that multichannel, spectrally aligned features produced by MEWT are particularly suitable for a compact convolutional architecture such as EEGNet on this ASD–EEG dataset and that the main limitation of the original EWT pipeline lies in its univariate, per-channel implementation. The clearer gap between MEWT-EEGNet and EWT-EEGNet is mainly attributed to cross-electrode spectral consistency. With univariate EWT, sub-band boundaries are estimated independently per channel, so the same sub-band index can represent slightly different frequency content across electrodes, increasing feature variability and weakening multichannel learning. In contrast, MEWT derives boundaries from the trial-level multichannel spectrum and applies a shared filter bank across all electrodes, producing spectrally aligned sub-bands that better match EEGNet's multichannel spatial–temporal modeling.

The smaller margin over EMD-EEGNet is consistent with both methods being adaptive, but MEWT is typically more controlled and repeatable because it enforces a fixed five-band partition with multichannel-derived boundaries, whereas EMD can exhibit mode variability and mode-mixing across segments. We also link this mechanism to Fig. 3 (a)–(d), where MEWT reconstruction shows a more regular oscillatory waveform and reduced transient excursions relative to band-pass outputs, supporting a cleaner and more stable input for EEGNet. Even so, the scope of the present work is intentionally narrow; only the MEWT with the EEGNet pipeline is trained and analyzed in detail, and comparisons to EWT and EMD-based methods are made at the benchmark level using previously published results. Future studies will retrain all three feature families (EWT, EMD, and MEWT) under exactly the same segmentation and cross-validation protocol, extend the evaluation to additional classifiers (e.g., SVM-RBF or shallow CNNs, and transformers), and test the MEWT with the EEGNet pipeline on larger and more heterogeneous cohorts to assess how well the observed gains carry over to new subjects and recording conditions.

Because the EWT with EEGNet and EMD with EEGNet results were taken from previously published studies, cross-study comparisons may still be influenced by differences in the sample construction stage (segmentation/epoching), such as window length, overlap, and segmentation rules. To strengthen fairness, we explicitly matched the key controllable factors: the same dataset, a subject-wise cross-validation protocol, the same EEGNet-style classifier family, the same number of training epochs, and the same reporting metrics. Consequently, the remaining discrepancy primarily reflects the impact of segmentation choices in the referenced studies; therefore, we interpret this benchmark as a contextual comparison rather than a strict head-to-head leaderboard [9].

A similar caution applies to computational efficiency. Beyond classification performance, we assessed computational efficiency to support the pipeline's suitability for screening in resource-constrained settings by reporting model complexity, EEGNet inference latency, and the computational cost of the signal-representation stage. The EEGNet implementation is lightweight; with a 16-channel × 1000-sample input, it contains 3,139 trainable parameters, implying a small memory footprint. We emphasize that end-to-end runtime is also affected by the segmentation setup: MEWT uses 2-s segments with 50% overlap (batch size 64), whereas the EWT/EMD baselines use 4-s segments with 50% overlap, making raw comparisons of total training or inference time potentially biased by different segment lengths. Therefore, we report more comparable metrics per-segment inference latency and per-segment representation runtime (and throughput at the chosen batch size) to enable transparent assessment of computational trade-offs and deployment-time cost estimation, particularly given that prior EWT/EMD studies do not consistently report runtime metrics.

Although the subject-wise cross-validation results are strong, the study can be further strengthened by testing the pipeline on larger, more diverse datasets and across different recording/segmentation settings to confirm generalization better. The subject-wise 5-fold evaluation is appropriate for preventing information leakage, but additional validation (e.g., external validation) could provide a more comprehensive view of inter-individual variability. To reduce degrees of freedom, we used a fixed preprocessing configuration (0.5–40 Hz band-pass) and a fixed segmentation strategy (2-s windows, 50% overlap) across all folds. Although the fold-to-fold variation is small, we did not conduct an exhaustive sensitivity analysis across learning rates, batch sizes, or MEWT parameters; this is now explicitly stated as a limitation, consistent with recent discussions on how preprocessing and partitioning choices can influence decoding performance [36], [39]. Consistent with this, misclassifications in our current cohort are infrequent and remain approximately balanced

**Corresponding author:** Melinda, melinda@usk.ac.id, Department of Electrical and Computer Engineering, Universitas Syiah Kuala, Banda Aceh, Indonesia.
**Digital Object Identifier (DOI):** https://doi.org/10.35882/ijeeemi.v8i1.313

between false positives and false negatives (Table 2 and Fig. 4), suggesting no systematic bias toward either class. However, the small cohort size limits statistically robust subject-level or segment-level error characterization, such as determining whether errors cluster in specific participants or recur in particular segment types; this will be a focused direction for future work as larger multi-site datasets become available. In addition, the current comparison with EWT and EMD is benchmark-based, as in prior studies, so retraining all methods under a fully identical protocol would enable a fairer comparison, and interpretability analyses could be added to better link the results to neurophysiological meaning and practical applicability. Additionally, sex distribution and detailed diagnostic instruments for the ASD cohort were inconsistently documented in the source dataset, limiting demographic and clinical subgroup analyses.

These findings indicate that using MEWT to align frequency-band boundaries across channels can improve multichannel EEG representations and work effectively with compact classifiers such as EEGNet. The consistently high performance under subject-wise validation also suggests that the proposed pipeline has potential as a computationally efficient screening-oriented model, particularly in resource-constrained settings [9]. In addition, this study highlights the importance of validation design, especially subject-wise grouping as a minimum standard, to avoid biased evaluation and to better reflect real-world performance. Overall, the results motivate future work to adopt multichannel decomposition/denoising and to test it on larger, more diverse cohorts under standardized protocols to support the development of more robust and transferable EEG-based ASD biomarkers [41]. Building a deployable screening tool on these findings, several requirements extend beyond predictive performance alone. These include robust, automated signal-quality assessment and artifact detection; standardized acquisition procedures to ensure reproducible measurements across operators and sites; and clinician-oriented interfaces that present outputs in an interpretable and actionable manner. Moreover, prospective validation on representative, real-world cohorts is essential to quantify performance under operational conditions, including variation in demographics, comorbidities, and recording environments [42],[43]. Equally important are ethical, regulatory, and governance considerations. Clinically, both false reassurance and false alarms carry non-trivial consequences, necessitating transparent communication of model uncertainty, intended use, and limitations, alongside appropriate clinical oversight and escalation pathways. Prior to any diagnostic deployment, compliance with applicable regulatory frameworks and rigorous data-governance provisions covering privacy, security, consent, auditability, and ongoing performance monitoring would be required to ensure safe and responsible use [44].

## V. Conclusion

This study presents an ASD–EEG classification pipeline that integrates the Multivariate Empirical Wavelet Transform (MEWT) with EEGNet using 16-channel EEG recordings, segmented into 2-s windows with 50% overlap and resampled to a 16 × 1000 input format. The proposed model achieved a mean test accuracy of 98.35%, with a precision 98.23%, a recall 98.45%, an F1-score 98.34%, a specificity 98.24%, and an AUC 99.86% across five cross-validation folds, while confusion-matrix analysis showed consistently low and balanced false positives and false negatives. A one-sample t-test against the 50% chance level confirmed that all metrics were highly significant ($p < 0.0001$). When compared on the same dataset, the MEWT with the EEGNet approach outperformed EWT with the EEGNet (95.08%) and slightly improved upon EMD with the EEGNet (97.99%), demonstrating the effectiveness of multichannel, spectrally aligned features for ASDEEG classification. Although the results indicate high accuracy, stability, and balanced sensitivity–specificity, the study is limited by a small, single-site dataset and a single deep-learning architecture, suggesting the need for future validation in larger cohorts and with additional classifiers.

## References

[1] M. Milovanovic and R. Grujicic, “Electroencephalography in Assessment of Autism Spectrum Disorders: A Review,” *Frontiers in Psychiatry*, vol. 12. Frontiers Media S.A., Sep. 29, 2021. doi: 10.3389/fpsyt.2021.686021.

[2] S. Peng, R. Xu, X. Yi, X. Hu, L. Liu, and L. Liu, “Early Screening of Children With Autism Spectrum Disorder Based on Electroencephalogram Signal Feature Selection With L1-Norm Regularization,” *Front. Hum. Neurosci.*, vol. 15, Jun. 2021, doi: 10.3389/fnhum.2021.656578.

[3] W. S. Neo, D. Foti, B. Keehn, and B. Kelleher, “Resting-state EEG power differences in autism spectrum disorder: a systematic review and meta-analysis,” *Transl. Psychiatry*, vol. 13, no. 1, pp. 1–14, 2023, doi: 10.1038/s41398-023-02681-2.

[4] L. Bogéa Ribeiro and M. da Silva Filho, “Systematic Review on EEG Analysis to Diagnose and Treat Autism by Evaluating Functional Connectivity and Spectral Power,” *Neuropsychiatr. Dis. Treat.*, vol. 19, pp. 415–424, 2023, doi: 10.2147/NDT.S394363.

[5] M. Melinda, F. Arnia, A. Yafi, N. Afny, C. Andryani, and I. K. A. Enriko, “Design and Implementation of Mobile Application for CNN-Based EEG Identification of Autism Spectrum Disorder,” vol. 14, no. 1, 2024.

[6] P. Babaeeghazvini, L. M. Rueda-Delgado, J. Gooijers, S. P. Swinnen, and A. Daffertshofer, “Brain Structural and Functional Connectivity: A Review of Combined Works of Diffusion Magnetic Resonance Imaging and Electro-Encephalography,” *Front. Hum. Neurosci.*, vol. 15, no. October, 2021, doi:

**Corresponding author:** Melinda, melinda@usk.ac.id, Department of Electrical and Computer Engineering, Universitas Syiah Kuala, Banda Aceh, Indonesia.
**Digital Object Identifier (DOI):** https://doi.org/10.35882/ijeeemi.v8i1.313

10.3389/fnhum.2021.721206.

[7] B. Yildirim, O. Ulkir, M. Kaya, A. K. Singh, and S. Krishnan, "Trends in EEGsignal feature extraction applications.Front. Artif. Intell.5:1072801.doi: 10.3389/frai.2022.1072801," 2023.

[8] M. T. Sadiq *et al.*, "Motor Imagery EEG Signals Decoding by Multivariate Empirical Wavelet Transform-Based Framework for Robust Brain-Computer Interfaces," *IEEE Access*, vol. 7, pp. 171431–171451, 2019, doi: 10.1109/ACCESS.2019.2956018.

[9] M. Melinda *et al.*, "Feature-Based EEG Classification: A Comparative Study of EMD and EWT with EEGNet and Shallow FBCSP ConvNet," *IEEE Access*, 2025, doi: 10.1109/ACCESS.2025.3625234.

[10] K. Das, A. Mondal, N. Phukan, and R. B. Pachori, "7 - Multivariate adaptive signal decomposition techniques and their applications to EEG signal processing: An introduction," in *Advances in Neural Engineering*, A. S. El-Baz and J. S. B. T.-S. P. S. Suri, Eds., Academic Press, 2025, pp. 137–161. doi: https://doi.org/10.1016/B978-0-323-95437-2.00011-2.

[11] C.-G. Lucas and J. Gilles, "Multidimensional empirical wavelet transform," Dec. 2024, [Online]. Available: http://arxiv.org/abs/2405.06188

[12] V. J. Lawhern, A. J. Solon, N. R. Waytowich, S. M. Gordon, C. P. Hung, and B. J. Lance, "EEGNet: a compact convolutional neural network for EEG-based brain–computer interfaces," *J. Neural Eng.*, vol. 15, no. 5, p. 056013, 2018, doi: 10.1088/1741-2552/aace8c.

[13] S. S. Bhat, P. P., K. V S., A. Raghunandan, and B. R. Mohan, "Comparative Performance Evaluation of Web-Based Book Recommender Systems," in *2022 6th International Conference on Trends in Electronics and Informatics (ICOEI)*, 2022, pp. 985–991. doi: 10.1109/ICOEI53556.2022.9777116.

[14] B. Liu, H. Chang, K. Peng, and X. Wang, "An End-to-End Depression Recognition Method Based on EEGNet," *Front. Psychiatry*, vol. 13, no. March, pp. 1–9, 2022, doi: 10.3389/fpsyt.2022.864393.

[15] M. Muliyadi, M. Melinda, Y. Away, and S. Gazali, "Comparative Analysis of Normal and ASD EEG Data Using Hjorth Parameters," in *2025 7th International Congress on Human-Computer Interaction, Optimization and Robotic Applications (ICHORA)*, 2025, pp. 1–6. doi: 10.1109/ICHORA65333.2025.11017066.

[16] M. Melinda, P. D. Purnamasari, F. Fahmi, E. Sinulingga, M. Muliyadi, and I. A. Yamin, "Innovative Portable Quantitative EEG Data Acquisition Based Cyton Biosensing Board using PSD Analysis," in *2024 10th International Conference on Smart Computing and Communication (ICSCC)*, 2024, pp. 631–636. doi: 10.1109/ICSCC62041.2024.10690827.

[17] M. Jannatul Ferdous, M. Sujan Ali, M. Ekramul Hamid, and M. Khademul Islam Molla, "A Comparison of Butterworth Band pass Filter and Discrete Wavelet Transform Filter for the Suppression of Ocular Artifact from EEG Signal," *Int. J. Res. Eng. Technol.*, vol. 1, [Online]. Available: http://www.ijretjournal.org

[18] S. P. D. Sriyanto, A. R. Puhi, and C. H. G. Sibuea, "The performance of Butterworth and Wiener filter for earthquake signal enhancement: a comparative study," *J. Seismol.*, vol. 27, no. 1, pp. 219–232, Feb. 2023, doi: 10.1007/s10950-022-10123-7.

[19] I. F. Rahman *et al.*, "EEG Performance Signal Analysis for Diagnosing Autism Spectrum Disorder Using Butterworth and Empirical Mode Decomposition," *J. Electron. Electromed. Eng. Med. Informatics*, vol. 7, no. 3, pp. 925–939, 2025, doi: 10.35882/jeeemi.v7i3.788.

[20] R. Kessler, A. Enge, and M. A. Skeide, "How EEG preprocessing shapes decoding performance," *Commun. Biol.*, vol. 8, no. 1, 2025, doi: 10.1038/s42003-025-08464-3.

[21] P. Arpaia *et al.*, "A Systematic Review of Techniques for Artifact Detection and Artifact Category Identification in Electroencephalography from Wearable Devices," *Sensors*, vol. 25, no. 18, pp. 1–59, 2025, doi: 10.3390/s25185770.

[22] B. S. Falih, M. K. Sabir, and A. Aydın, "Impact of Sliding Window Overlap Ratio on EEG-Based ASD Diagnosis Using Brain Hemisphere Energy and Machine Learning," *Appl. Sci.*, vol. 14, no. 24, pp. 1–20, 2024, doi: 10.3390/app142411702.

[23] L. A. Moctezuma, T. Abe, and M. Molinas, "Two-dimensional CNN-based distinction of human emotions from EEG channels selected by multi-objective evolutionary algorithm," *Sci. Rep.*, vol. 12, no. 1, pp. 1–15, 2022, doi: 10.1038/s41598-022-07517-5.

[24] G. Brookshire *et al.*, "Data leakage in deep learning studies of translational EEG," *Front. Neurosci.*, vol. 18, 2024, doi: 10.3389/fnins.2024.1373515.

[25] F. Del Pup, A. Zanola, L. F. Tshimanga, A. Bertoldo, L. Finos, and M. Atzori, "The role of data partitioning on the performance of EEG-based deep learning models in supervised cross-subject analysis: A preliminary study," *Comput. Biol. Med.*, vol. 196, no. PA, p. 110608, 2025, doi: 10.1016/j.compbiomed.2025.110608.

[26] J. Gilles, "Empirical wavelet transform," *IEEE Trans. Signal Process.*, vol. 61, no. 16, pp. 3999–4010, 2013, doi: 10.1109/TSP.2013.2265222.

[27] R. K. Tripathy, S. K. Ghosh, P. Gajbhiye, and U. R. Acharya, "Development of automated sleep stage classification system using multivariate projection-based fixed boundary empirical wavelet transform and entropy features extracted from multichannel eeg signals," *Entropy*, vol. 22, no. 10, pp. 1–23,

**Corresponding author:** Melinda, melinda@usk.ac.id, Department of Electrical and Computer Engineering, Universitas Syiah Kuala, Banda Aceh, Indonesia.
**Digital Object Identifier (DOI):** https://doi.org/10.35882/ijeeemi.v8i1.313

Oct. 2020, doi: 10.3390/e22101141.

[28] I. Siviero, L. Brusini, G. Menegaz, and S. F. Storti, "Motor-imagery EEG signal decoding using multichannel-empirical wavelet transform for brain computer interfaces," in *2022 IEEE-EMBS International Conference on Biomedical and Health Informatics (BHI)*, 2022, pp. 1–4. doi: 10.1109/BHI56158.2022.9926766.

[29] "R. K. Tripathy, S. K. Ghosh, P. Gajbhiye, and U. R. Acharya, "Development of automated sleep stage classification system using multivariate projection-based fixed boundary empirical wavelet transform and entropy features extracted from multichannel eeg signals," Entropy, vol. 22, no. 10, pp. 1–23, Oct. 2020, doi: 10.3390/e22101141."

[30] V. P. Balam, "Automated EEG signal processing: A comprehensive investigation into preprocessing techniques and sub-band extraction for enhanced brain-computer interface applications," *J. Neurosci. Methods*, vol. 424, p. 110561, 2025, doi: https://doi.org/10.1016/j.jneumeth.2025.110561.

[31] M. T. Sadiq *et al.*, "Motor Imagery EEG Signals Decoding by Multivariate Empirical Wavelet Transform-Based Framework for Robust Brain-Computer Interfaces," *IEEE Access*, vol. 7, no. Mi, pp. 171431–171451, 2019, doi: 10.1109/ACCESS.2019.2956018.

[32] O. Singh and R. K. Sunkaria, "An empirical wavelet transform based approach for multivariate data processing application to cardiovascular physiological signals," *Bio-Algorithms and Med-Systems*, vol. 14, no. 4, pp. 1–7, 2018, doi: 10.1515/bams-2018-0030.

[33] V. J. Lawhern, A. J. Solon, N. R. Waytowich, S. M. Gordon, C. P. Hung, and B. J. Lance, "EEGNet: A compact convolutional neural network for EEG-based brain-computer interfaces," *J. Neural Eng.*, vol. 15, no. 5, Jul. 2018, doi: 10.1088/1741-2552/aace8c.

[34] C. M. Köllőd, A. Adolf, K. Iván, G. Márton, and I. Ulbert, "Deep Comparisons of Neural Networks from the EEGNet Family," *Electron.*, vol. 12, no. 12, pp. 1–15, 2023, doi: 10.3390/electronics12122743.

[35] Y. Jung and J. Hu, "A K-fold averaging cross-validation procedure," *J. Nonparametr. Stat.*, vol. 27, no. 2, pp. 167–179, Apr. 2015, doi: 10.1080/10485252.2015.1010532.

[36] J. White and S. D. Power, "k-Fold Cross-Validation Can Significantly Over-Estimate True Classification Accuracy in Common EEG-Based Passive BCI Experimental Designs: An Empirical Investigation," *Sensors*, vol. 23, no. 13, Jul. 2023, doi: 10.3390/s23136077.

[37] S. Prusty, S. Patnaik, and S. K. Dash, "SKCV: Stratified K-fold cross-validation on ML classifiers for predicting cervical cancer," *Front. Nanotechnol.*, vol. 4, no. August, pp. 1–12, 2022, doi: 10.3389/fnano.2022.972421.

[38] F. J. Ramírez-Arias *et al.*, "Evaluation of Machine Learning Algorithms for Classification of EEG Signals," *Technologies*, vol. 10, no. 4, Aug. 2022, doi: 10.3390/technologies10040079.

[39] M. Sokolova and G. Lapalme, "A systematic analysis of performance measures for classification tasks," *Inf. Process. Manag.*, vol. 45, no. 4, pp. 427–437, 2009, doi: https://doi.org/10.1016/j.ipm.2009.03.002.

[40] K. M. Sujon, R. Hassan, K. Choi, and A. Samad, "empirical evidence from advanced statistics , ML , and XAI for evaluating business predictive models," 2025.

[41] L. Billeci *et al.*, "An integrated EEG and eye-tracking approach for the study of responding and initiating joint attention in Autism Spectrum Disorders," *Sci. Rep.*, vol. 7, no. 1, pp. 1–13, 2017, doi: 10.1038/s41598-017-13053-4.

[42] M. K. Islam, A. Rastegarnia, and Z. Yang, "Methods for artifact detection and removal from scalp EEG: A review," *Neurophysiol. Clin. Neurophysiol.*, vol. 46, no. 4, pp. 287–305, 2016, doi: https://doi.org/10.1016/j.neucli.2016.07.002.

[43] F. Vaquerizo-Villar *et al.*, "An explainable deep-learning model to stage sleep states in children and propose novel EEG-related patterns in sleep apnea," *Comput. Biol. Med.*, vol. 165, p. 107419, 2023, doi: https://doi.org/10.1016/j.compbiomed.2023.107419.

[44] A. N. Vaidyam, H. Wisniewski, J. D. Halamka, M. S. Kashavan, and J. B. Torous, "Chatbots and Conversational Agents in Mental Health: A Review of the Psychiatric Landscape," *Can. J. Psychiatry*, vol. 64, no. 7, pp. 456–464, 2019, doi: 10.1177/0706743719828977.

## AUTHOR BIOGRAPHY

**Imam Fathur Rahman** was born on April 23, 2003, in Bireuen. He is currently pursuing a Master's degree in Electrical Engineering at Universitas Syiah Kuala, with a concentration in Biomedical Engineering. He completed his undergraduate studies in the Department of Electrical and Computer Engineering, Universitas Syiah Kuala, focusing on multimedia telecommunications engineering, with research specialization in EEG signal analysis. He actively engages in academic activities and continuously enhances his expertise in the field. Beyond his studies, he has gained experience as a teaching assistant and a digital signal processing laboratory assistant during his seventh semester. As part of the 2021 cohort, he strives to refine his skills and broaden his practical experience. His academic journey reflects a strong commitment to integrating theory and practice,

**Corresponding author:** Melinda, melinda@usk.ac.id, Department of Electrical and Computer Engineering, Universitas Syiah Kuala, Banda Aceh, Indonesia.
**Digital Object Identifier (DOI):** https://doi.org/10.35882/ijeeemi.v8i1.313

equipping him to contribute to future technological advancements. He can be contacted at: imamfr@mhs.usk.ac.id.

**Melinda** was born in Bireuen, Aceh, on June 10, 1979. She received a B.Eng degree from the Department of Electrical and Computer Engineering, Faculty of Engineering, Universitas Syiah Kuala, Banda Aceh, in 2002. She completed her master's degree at the Faculty of Electrical Department, University of Southampton, United Kingdom, with a concentration in field study of Radio Frequency Communication Systems in 2009. She has already completed her Doctoral degree at the Department of Electrical Engineering, Faculty of Engineering, Universitas Indonesia, in February 2018. She has been with the Department of Electrical Engineering, Faculty of Engineering, Universitas Syiah Kuala since 2002. She is also a member of IEEE. Her research interests include multimedia signal processing and fluctuation processing. She can be contacted at email: melinda@usk.ac.id

**Yunidar** was born in Banda Aceh, Aceh, on June 29, 1974. She has been a lecturer at the Faculty of Engineering, Department of Electrical and Computer Engineering, Syiah Kuala University, since March 2000. After completing her undergraduate education in Physics at Syiah Kuala University, Aceh, Indonesia, in 1997, she then obtained a master of Engineering (MT) degree in Optoelectrotechnics and Laser Applications from the University of Indonesia, Jakarta, Indonesia, in 2000. After which, she enrolled in a doctoral program in electrical and computer engineering at Syiah Kuala University and graduated in 2025. She is also a member of IEEE. Her research interests include the implementation of biomedical engineering and the use of sensors in biomedical applications, including multimedia. She can be contacted via email: yunidar@usk.ac.id.

**Dr. Nurlida Basir** is an Associate Professor at the Faculty of Science and Technology, Universiti Sains Islam Malaysia (USIM). She began her academic career at USIM in 2002 and has since been actively involved in teaching, research, and educational leadership. She holds a Diploma, a Bachelor's, and a Master's degree in Computer Science from Universiti Teknologi Malaysia (UTM), and earned her Ph.D. in Computer Science from the University of Southampton, United Kingdom. Her research interests span software engineering, cybersecurity malware detection, signal processing, and artificial intelligence. Her research has been extensively published in prominent academic journals and conference proceedings. Alongside her research, she is a dedicated educator, mentoring both undergraduate and postgraduate students in computer science. She is a member of the Institute of Electrical and Electronics Engineers (IEEE), reflecting her active participation in the global academic and research community. She can be contacted at nurlida@usim.edu.my.

**Aufa Rafik**i was born on April 20, 2003, in Banda Aceh. He received his Bachelor's degree in 2025 from the Department of Electrical and Computer Engineering, Universitas Syiah Kuala, where he focused on multimedia technology and the analysis of EEG signals. He is currently pursuing a Master's degree in Electrical Engineering at Universitas Syiah Kuala, with research interests centred on biomedical signal processing and deep learning for EEG based applications. During his undergraduate studies he served as a teaching assistant and programming laboratory assistant, gaining experience in both teaching and practical implementation. He is committed to strengthening his expertise in theory and applied research to contribute to tenchological developments in his field. He can be contacted at aufa35@mhs.usk.ac.id

.

**Corresponding author:** Melinda, melinda@usk.ac.id, Department of Electrical and Computer Engineering, Universitas Syiah Kuala, Banda Aceh, Indonesia.
**Digital Object Identifier (DOI):** https://doi.org/10.35882/ijeeemi.v8i1.313